Electronic Supplementary Information: Iridium(III) Azuliporphyrins

Timothy D. Lash,[a] Komal Pokharel,[a] Matthias Zeller[b] and Gregory M. Ferrence,[a]

[a] Department of Chemistry, Illinois State University, Normal, Illinois 61790-6160, USA.

E-mail: tdlash@ilstu.edu

[b] Department of Chemistry, Youngstown State University, One University Plaza, Youngstown, Ohio 44555, USA

Table of Contents

Page

Experimental Procedures

Azuliporphyrins **5a** and **5c** were prepared by literature procedures[S1,S2] and bis(1,5-cyclooctadiene)diiridium(II) dichloride was obtained from Alfa Aesar. All other reagents were purchased from Aldrich or Acros and were used without further purification. Proton and carbon-13 NMR spectra were obtained on a Bruker 500 MHz NMR spectrometer or a 400 MHz Varian Gemini NMR spectrometer at 25 °C unless otherwise indicated. Chemical shifts were recorded in parts per million (ppm) relative to $CDCl_3$ (residual chloroform at δ 7.26 ppm) or DMSO-d_5 (2.49 ppm) in proton NMR spectra and the $CDCl_3$ triplet at δ 77.23 ppm in carbon-13 NMR spectra. The UV-Vis spectra were collected on a Cary 100 Bio spectrophotometer. Melting points were obtained using a Mel-Temp apparatus and are uncorrected. Mass spectrometry data were obtained from the Mass Spectral Laboratory, School of Chemical Sciences, University of Illinois at Urbana-Champaign, and elemental analyses were obtained from the School of Chemical Sciences Microanalysis Laboratory at the University of Illinois.

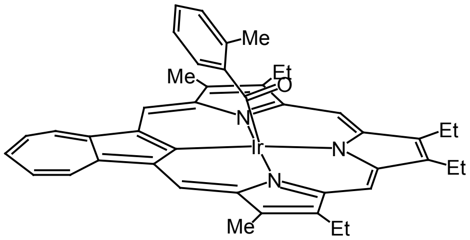

Iridium(III) complex 11a. $[Ir(COD)Cl]_2$ (42 mg, 0.062 mmol), azuliporphyrin **5a** (20 mg, 0.039 mmol) and anhydrous *o*-xylene (20 mL) were placed in a round bottom flask and refluxed with stirring under nitrogen overnight. The mixture was evaporated to dryness on a rotary evaporator and the residue treated with toluene (10 mL) and filtered. The filtrate was evaporated under reduced pressure and the residue purified on a silica gel column, eluting first with toluene and then with a 5% acetone-toluene mixture. The product was collected as a band that appeared dark green on the column but eluted as a reddish wine color. The solutions were evaporated to dryness and the residue was recrystallized from dichloromethane-hexanes to give the iridium(III) azuliporphyrin (3.0 mg, 0.0036 mmol, 9%) as dark crystals, mp >300 °C; UV-Vis ($CHCl_3$): λ_{max} (log ε) 374 (4.74), 444 (4.45), 521 nm (4.42); ^1H NMR (400 MHz, DMSO-d_6): δ -0.34 (3H, s), 1.49 (6H, t, J = 7.7 Hz), 1.55 (6H, t, J = 7.8 Hz), 3.22 (6H, s), 5.85-5.90 (2H, m), 6.25 (1H, t, J = 7.3 Hz), 7.34 (2H, t, J = 9.7 Hz), 7.67 (1H, t, J = 9.7 Hz), 8.31 (2H, s), 9.08 (2H, s), 9.24 (2H, d, J = 9.7 Hz); HRMS (EI) calcd for $C_{44}H_{42}IrN_3O$ m/z 821.2957, found 821.2961.

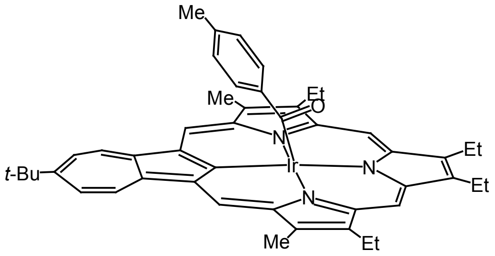

Iridium(III) complex 11c. Azuliporphyrin **5c** (40 mg, 0.070 mmol), [Ir(COD)Cl]$_2$ (71 mg, 0.106 mmol) and anhydrous *p*-xylene (40 mL) were reacted under the foregoing conditions. The product eluted from a silica column with 2-3% acetone-toluene. Recrystallization from dichloromethane-hexane gave **9c** (9.1 mg, 0.0104 mmol, 15%) as dark purple crystals, mp >300 ^{o}C; UV-Vis (CHCl$_3$): λ_{max} (log ε) 307 (sh, 4.29), 372 (4.76), 432 (sh, 4.42), 533 (4.50), 618 (4.01), 667 (sh, 3.93), 768 nm (sh, 3.29); IR (neat): $\nu_{C=O}$ 1637 cm^{-1}; ^{1}H NMR (500 MHz, CDCl$_3$): δ 1.49 (6H, t, *J* = 7.7 Hz), 1.57 (6H, t, *J* = 7.7 Hz), 1.58 (9H, s), 1.67 (3H, s), 2.92 (2H, d, *J* = 7.6 Hz), 2.99 (6H, s), 3.20-3.37 (6H, m), 3.39-3.47 (2H, m), 5.63 (2H, d, *J* = 7.6 Hz), 7.26 (2H, d, *J* = 10.4 Hz), 8.11 (2H, s), 8.21 (2H, s), 8.47 (2H, d, *J* = 10.4 Hz); ^{13}C NMR (500 MHz, CDCl$_3$, 50 ^{o}C): δ 10.5, 16.1, 17.8, 19.1, 19.5, 20.7, 31.3, 39.0, 96.9, 113.2, 113.2, 117.5, 124.1, 124.3, 125.5, 133.3, 137.19, 137.24, 138.1, 139.6, 140.5, 142.8, 147.1, 151.2, 155.4, 158.1, 171.3; HRMS (ESI) calcd for $C_{48}H_{50}IrN_3O$ + H *m/z* 878.3662, found 878.3661.

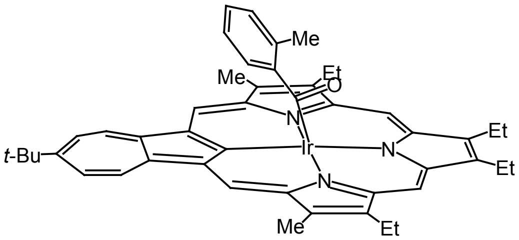

Iridium(III) complex 11d. Azuliporphyrin **5c** (40 mg, 0.070 mmol), [Ir(COD)Cl]$_2$ (71 mg, 0.106 mmol) and anhydrous *o*-xylene (40 mL) were reacted under the foregoing conditions. Recrystallization from dichloromethane-hexane gave **9d** (6.6 mg, 0.0075 mmol, 11%) as dark purple crystals, mp >300 ^{o}C; UV-Vis (CHCl$_3$): λ_{max} (log ε) 306 (sh, 4.35), 373 (4.82), 434 (sh, 4.50), 446 (4.50), 532 (4.52), 622 (4.07), 667 (4.01), 770 nm (sh, 3.38); IR (neat): $\nu_{C=O}$ 1636 cm^{-1}; ^{1}H NMR (500 MHz, CDCl$_3$): δ -0.54 (3H, s), 1.48 (6H, t, *J* = 7.7 Hz), 1.57 (6H, t, *J* = 7.6 Hz), 1.58 (9H, s), 2.69 (1H, d, *J* = 7.6 Hz), 3.01 (6H, s), 3.20-3.37 (6H, m), 3.38-3.46 (2H, m), 5.66-

5.71 (2H, m), 6.07 (1H, dt, *J* = 1.2, 7.3 Hz), 7.28 (2H, d, *J* = 10.7 Hz), 8.15 (2H, s), 8.35 (2H, s), 8.54 (2H, d, *J* = 10.7 Hz); ^{13}C NMR (500 MHz, $CDCl_3$): δ 10.5, 15.8, 16.3, 17.9, 19.1, 19.5, 31.3, 38.9, 96.9, 113.1, 118.6, 122.2, 124.0, 124.23, 124.26, 126.2, 126.8, 137.1, 137.3, 138.0, 140.3, 141.7, 142.7, 147.0, 150.8, 155.5, 158.0, 174.5; HRMS (ESI) calcd for $C_{48}H_{50}IrN_3O$ + H *m/z* 878.3662, found 878.3656.

Crystallographic Experimental Details of 11c. X-ray quality crystals of **11c** were obtained by vapor diffusion of petroleum ether into a dichloromethane solution of the compound to yield red plates. The crystals were suspended in mineral oil at ambient temperature and the best available crystal was selected. The crystals under investigation were heavily intergrown and no unique single crystal of sufficient size could be obtained from the crystals at hand. Multiple crystals and fragments were screened for diffraction intensity and number of crystal moieties present. As a compromise between crystal quality on the one hand and crystal size and diffraction intensity on the other, a 0.15 x 0.12 x 0.09 mm fragment, extracted out of one of the larger clusters and with only a moderate number of intergrown crystallites, was ultimately chosen for a full data collection. The mineral oil coated fragment was mounted on a 50 mm MicroMesh MiTeGen Micromount and transferred to a Bruker AXS SMART APEX CCD X-ray diffractometer. The X-ray diffraction data were collected at -173ºC using Mo-K_α (λ = 0.71073 Å) radiation. Data collection and cell refinement were performed using SMART and SAINT+, respectively.[S3] To handle the presence of multiple crystallites in the selected fragment, the orientation matrices for the three strongest components were identified using the program Cell Now, with the various components not being related by any obvious twin laws. All three components were integrated using SAINT+, resulting in the following reflection distributions and intensity statistics:

19534 data (8540 unique) involve domain 1 only, mean I/sigma 3.7
11980 data (5422 unique) involve domain 2 only, mean I/sigma 4.0
8794 data (4185 unique) involve domain 3 only, mean I/sigma 0.2
23398 data (13935 unique) involve 2 domains, mean I/sigma 3.9
7330 data (5482 unique) involve 3 domains, mean I/sigma 5.4

The unit cell parameters were obtained from a least-squares refinement of 6423 centered reflections from the first of the three components. Compound **11c** was found to crystallize in the monoclinic crystal system with the following unit cell parameters: a = 13.010(3) Å, b = 15.894(3) Å, c = 18.593(4) Å, β = 93.258(3)˚, Z = 4. The structure solved in the space group $P2_1/c$ (no. 14). The total number of reflections given (11245) is before merging of the data in TWINABS. The R_{int} value (0.1072) given is for these reflections and is based on agreement between observed single and composite intensities and those calculated from refined unique intensities and twin fractions before merging. Of the reflections collected, 8624 were unique, and 5804 were observed $F_o^2 > 2\ \sigma(F_o^2)$. Limiting indicies were as follows: $-16 \leq h \leq 16$, $0 \leq k \leq 20$, $0 \leq l \leq 24$. Data reduction were accomplished using SAINT.[S3] The data were corrected for absorption using the TWINABS procedure.[S4] Solution and data analysis were performed using the WinGX software package.[S5] The structure of **11c** was solved by charge-flipping methods using the program SUPERFLIP[S6] with only the non-overlapping reflections of the first component. The first component was chosen based on the lower number of overlapping reflections with moieties 2 and 3, despite the slightly lower diffraction intensities of this moiety when compared to the second moiety. All overlapping reflections were ignored in the refinement.

The refinement was completed using the program SHELX-97.[S7] The 1 0 0 and 0 1 1 reflections were obscured by the beamstop, so they were eliminated from the refinement using the OMIT SHELX card. All non-H atoms were refined anisotropically. All H atoms were included in the refinement in the riding-model approximation (C--H = 0.95, 0.98 and 0.99Å for Ar--H, CH_3 and CH_2; U_{iso} (H) = $1.2U_{\text{eq}}$(C) except for methyl groups, where U_{iso} (H) = $1.5U_{\text{eq}}$(C)).

The *tert*-butyl moiety was refined with positional disorder as two sets of methyl groups with 0.65671:0.34329 occupancy ratio. To achieve isotropic refinement of the lower occupancy PART of these methyl groups, it was necessary to apply EADP restraints to tie them to their corresponding higher occupancy partners.

Full-matrix least-squares refinement on F^2 led to convergence, $(\Delta/\sigma)_{\text{max}} = 0.000$, $(\Delta/\sigma)_{\text{mean}} = 0.0000$, with $R_1 = 0.0553$ and $wR_2 = 0.1051$ for 5804 data with $F_o^2 > 2\sigma(F_o^2)$ using 0 restraints and 495 parameters. A final difference Fourier synthesis showed features in the range of $\Delta\rho_{max}$ = 1.876 e$^-$/Å^3 to $\Delta\rho_{min}$ = -1.275 e$^-$/Å^3, which were deemed of no chemical significance. Molecular diagrams were generated using ORTEP-3.[S8]

References

S1 (a) T. D. Lash and S. T. Chaney, *Angew. Chem. Int. Ed.*, 1997, **36**, 839-840. (b) T. D. Lash, D. A. Colby, S. R. Graham and S. T. Chaney, *J. Org. Chem.*, 2004, **69**, 8851-8864.

S2 T. D. Lash, J. A. El-Beck and G. M. Ferrence, *J. Org. Chem.*, 2007, **72**, 8402-8415.

S3 Bruker, *APEX2 v2008.2-4*, Bruker AXS Inc., Madison, Wisconsin, USA, 2008.

S4 G. M. Sheldrick, G. M. (2007). TWINABS. University of Göttingen, Germany.

S5 L. J. Farrugia, *J. Appl. Crystallogr.*, 1999, **32**, 837-838.

S6 L. Palatinus and G. Chapuis, *J. Appl. Cryst.*, 2007, **40**, 786-790.

S7 G. M. Sheldrick, *Acta Cryst.*, 2008, **A64**, 112-122.

S8 L. J. Farrugia, *J. Appl. Crystallogr.*, 1997, **30**, 565.

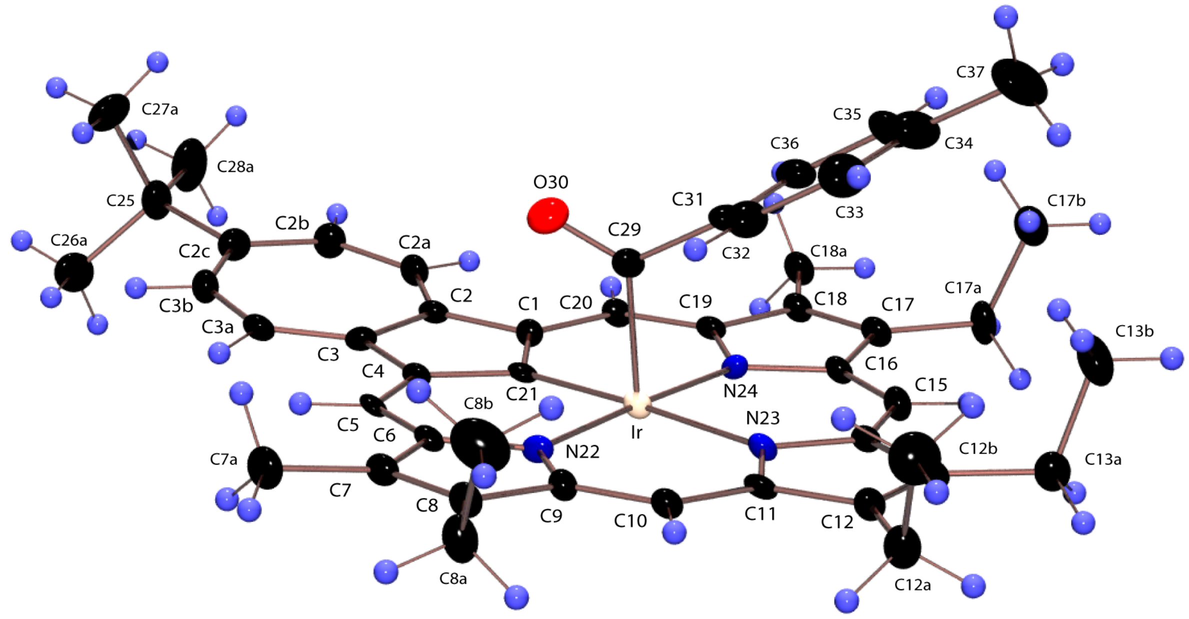

Figure S1. Color POV-Ray rendered ORTEP III drawing (30% probability level, hydrogen atoms drawn arbitrarily small) of acyliridium(III) azuliporphyrin **11c**.

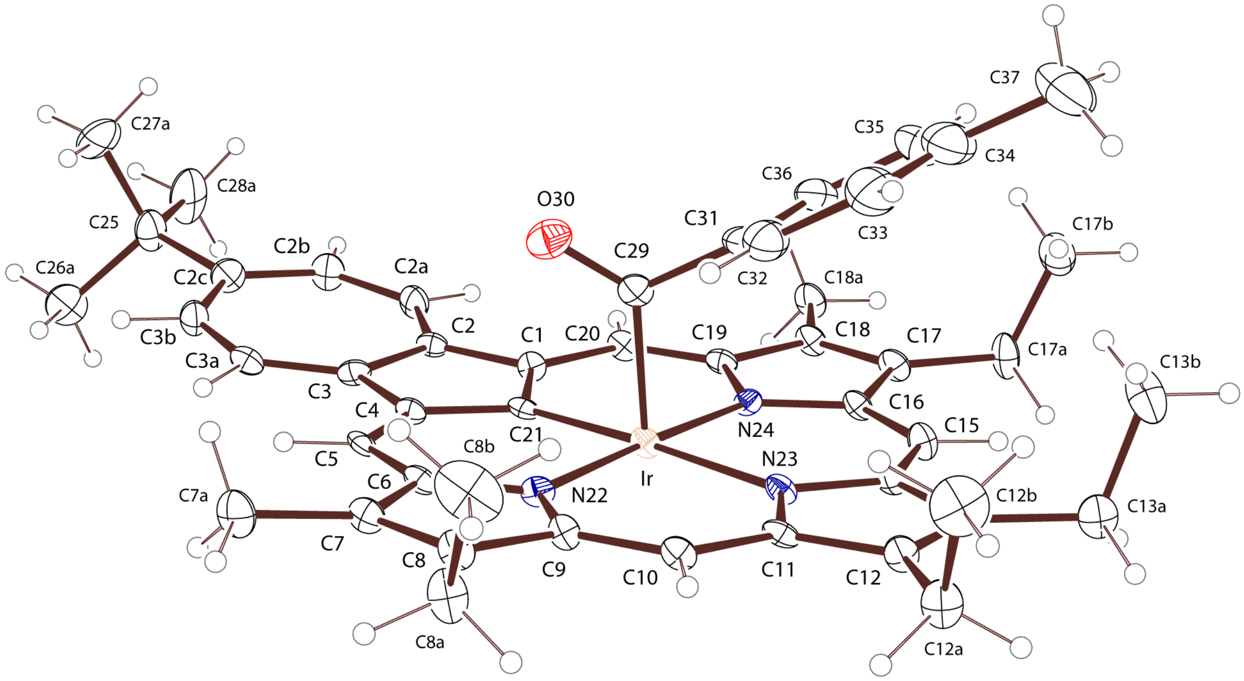

Figure S2. ORTEP III drawing (30% probability level, hydrogen atoms drawn arbitrarily small) of iridium(III) derivative **11c**.

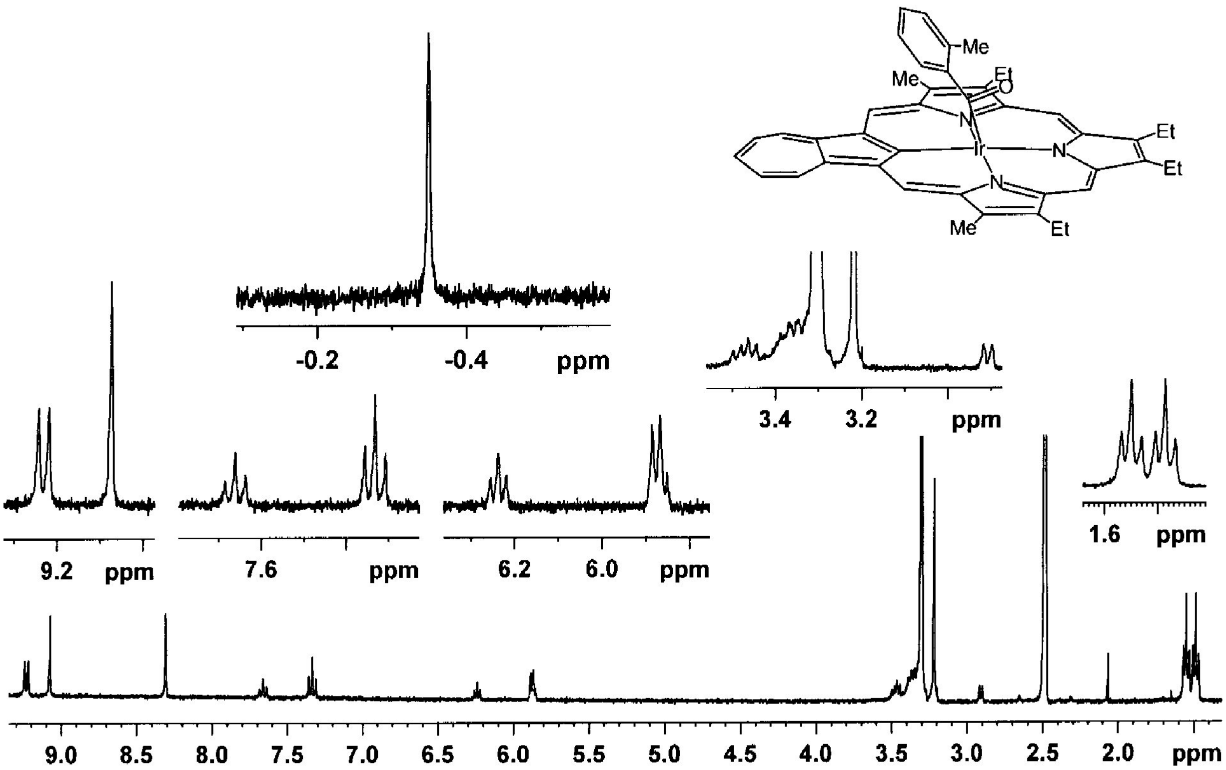

Figure S3. 400 MHz proton NMR spectrum of **11a** in DMSO-d_6.

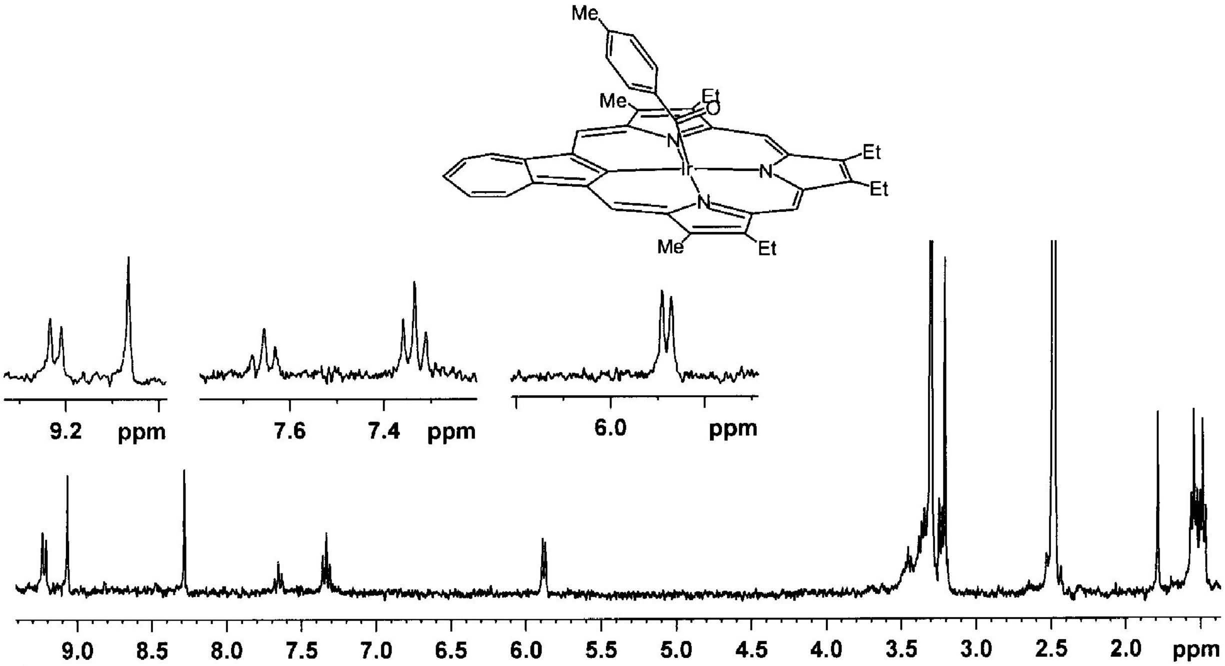

Figure S4. 400 MHz proton NMR spectrum of **11b** in DMSO-d_6.

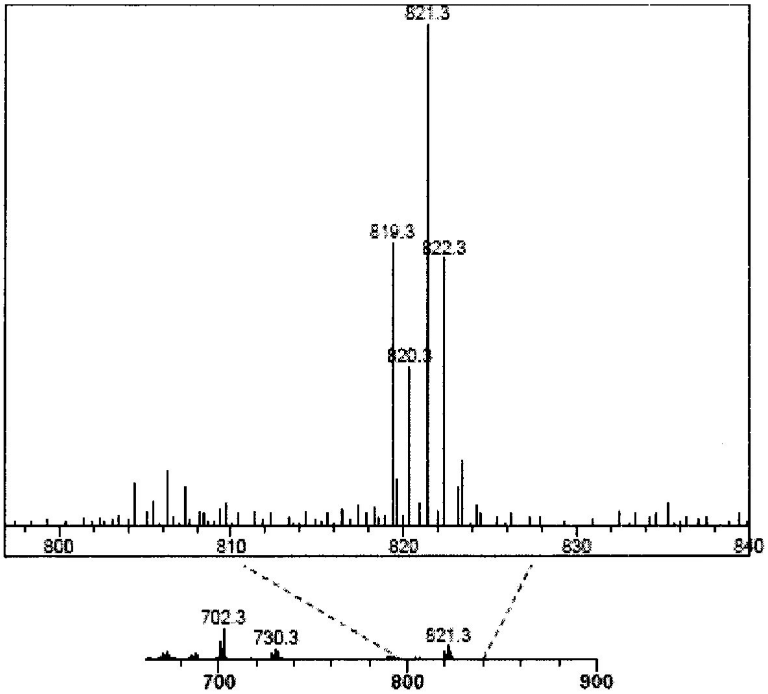

Figure S5. Electron impact mass spectrum of **11a**.

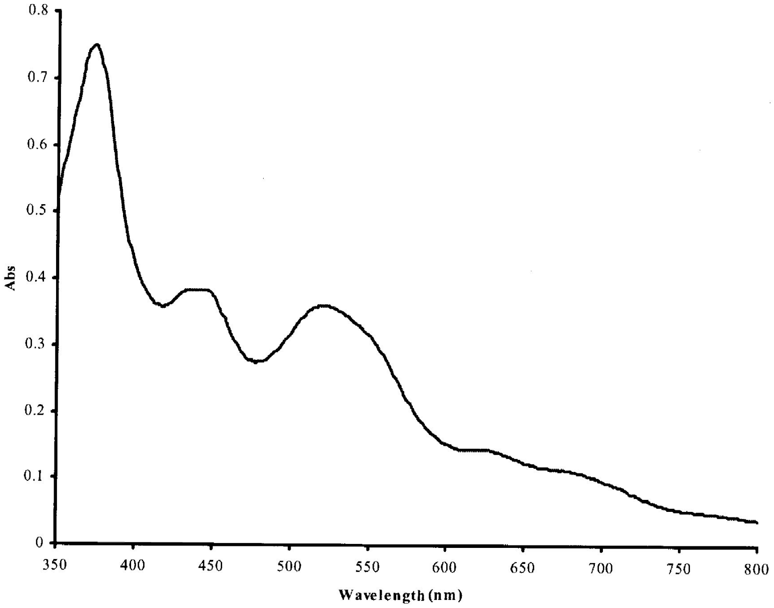

Figure S6. UV-Vis spectrum of **11a** in chloroform.

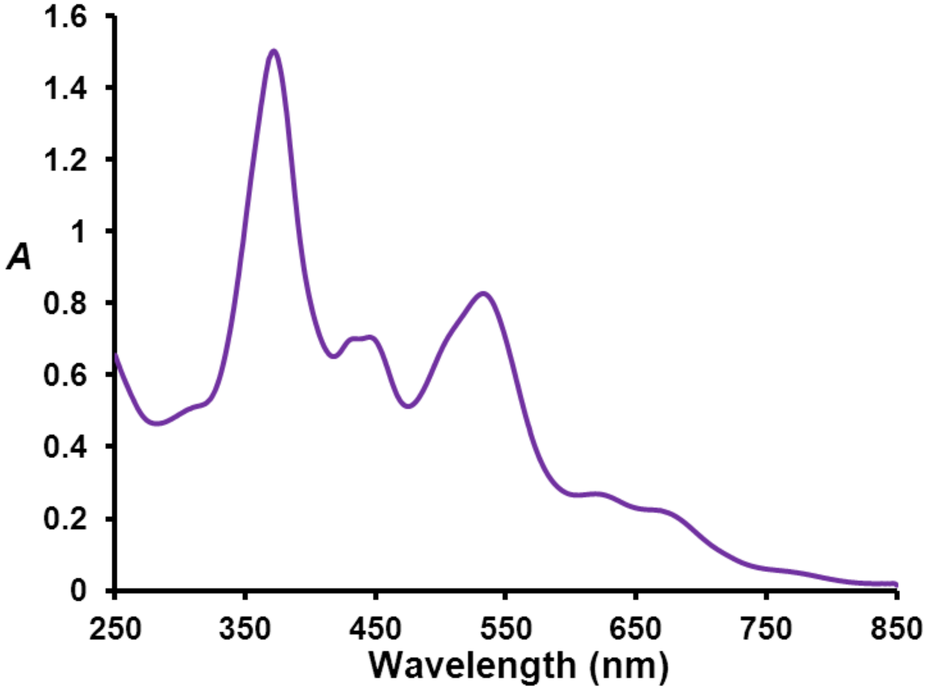

Figure S7. UV-Vis spectrum of **11c** in chloroform.

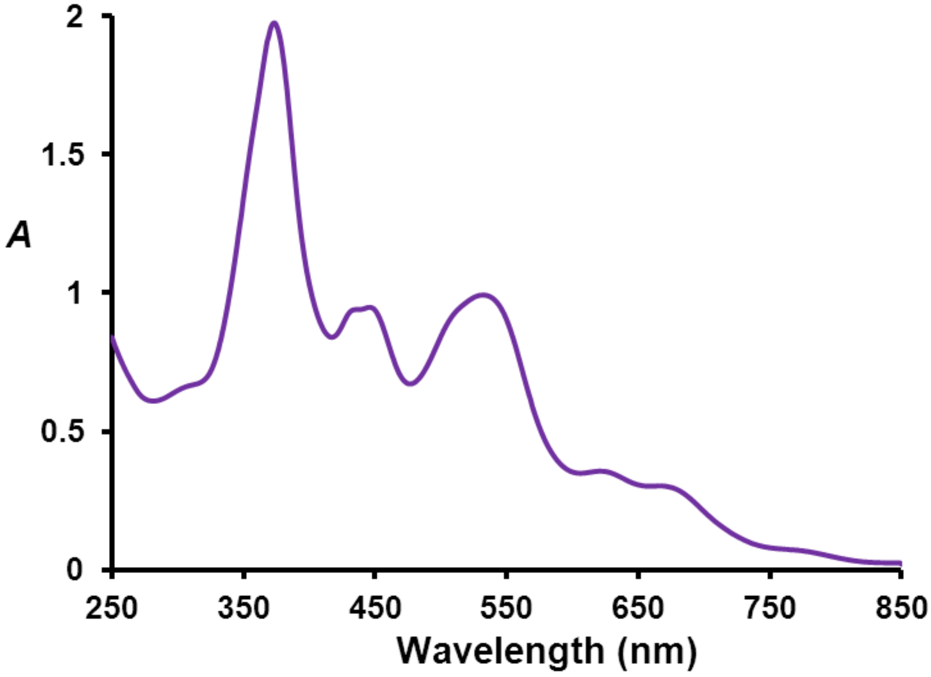

Figure S8. UV-Vis spectrum of **11d** in chloroform.

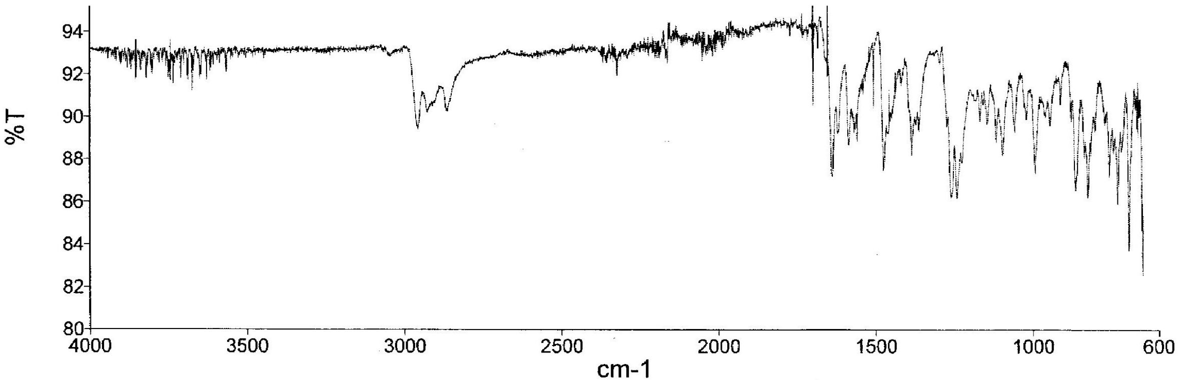

Figure S9. IR spectrum for iridium(III) azuliporphyrin **11c**.

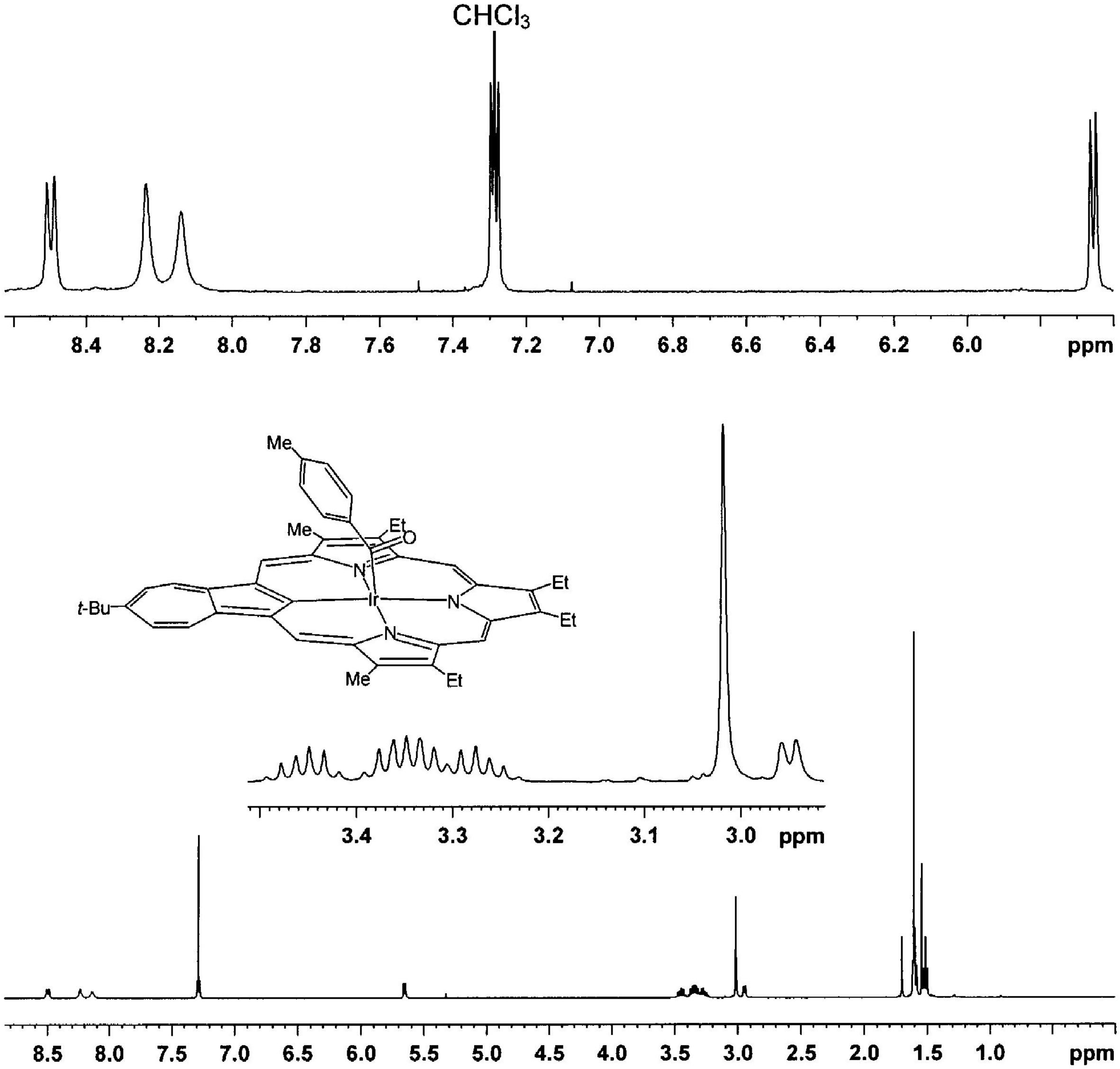

Figure S10. 500 MHz proton NMR spectrum of iridium(III) complex **11c** in $CDCl_3$ at 25 °C.

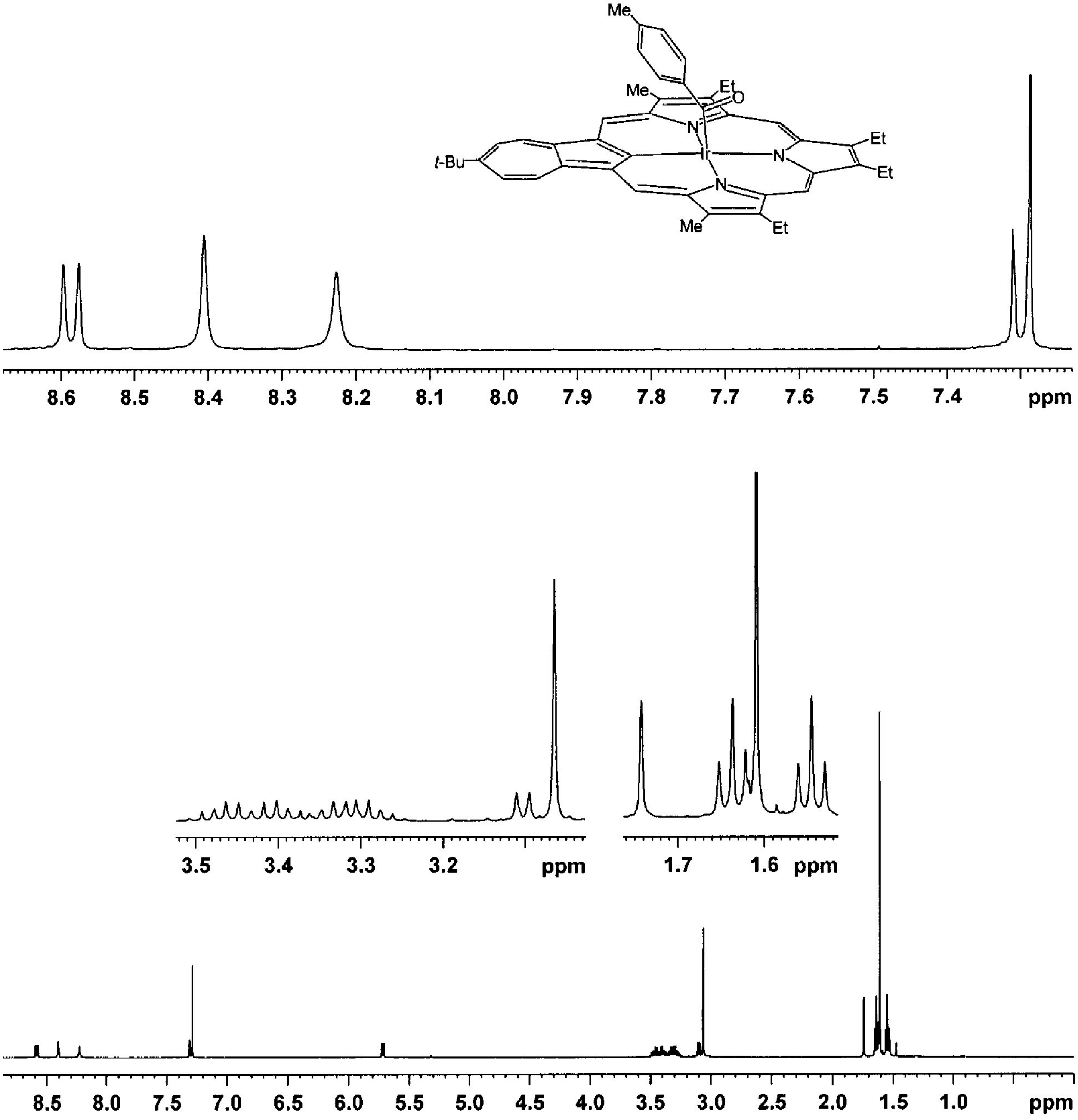

Figure S11. 500 MHz proton NMR spectrum of iridium(III) complex **11c** in $CDCl_3$ at 50 °C.

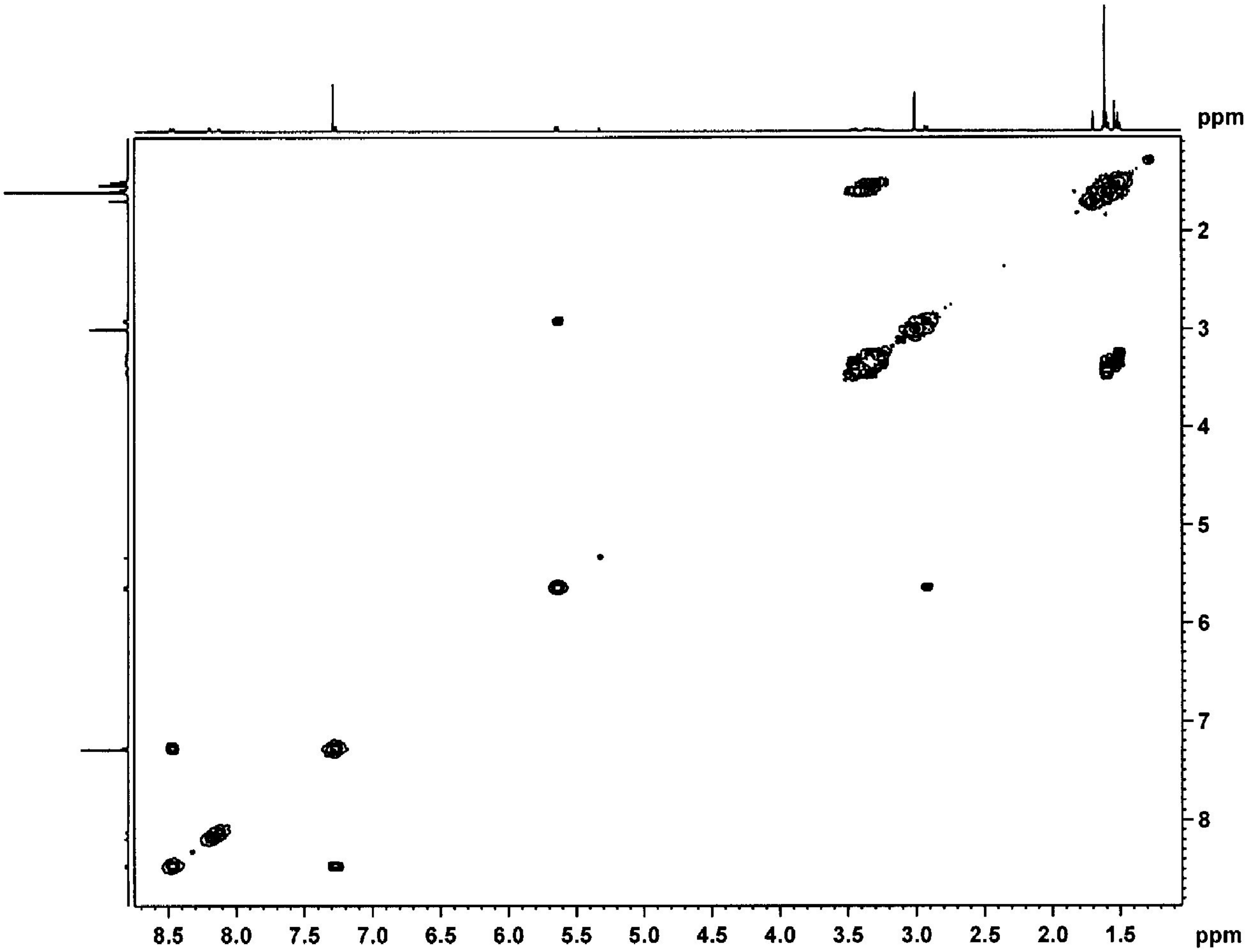

Figure S12. ^{1}H-^{1}H COSY NMR spectrum of iridium(III) complex **11c** in $CDCl_3$.

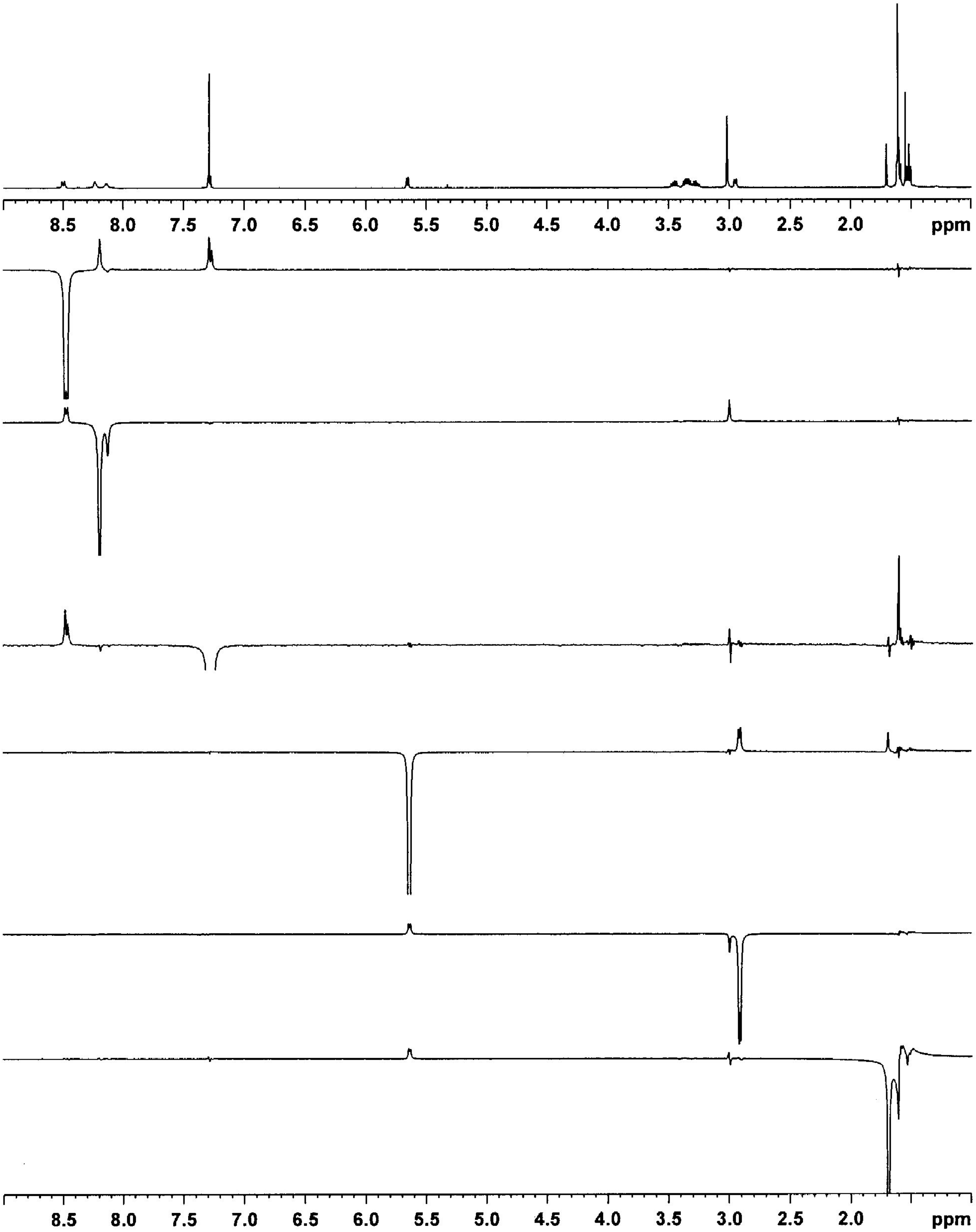

Figure S13. Selected nOe difference proton NMR spectra of iridium(III) complex **11c** in $CDCl_3$.

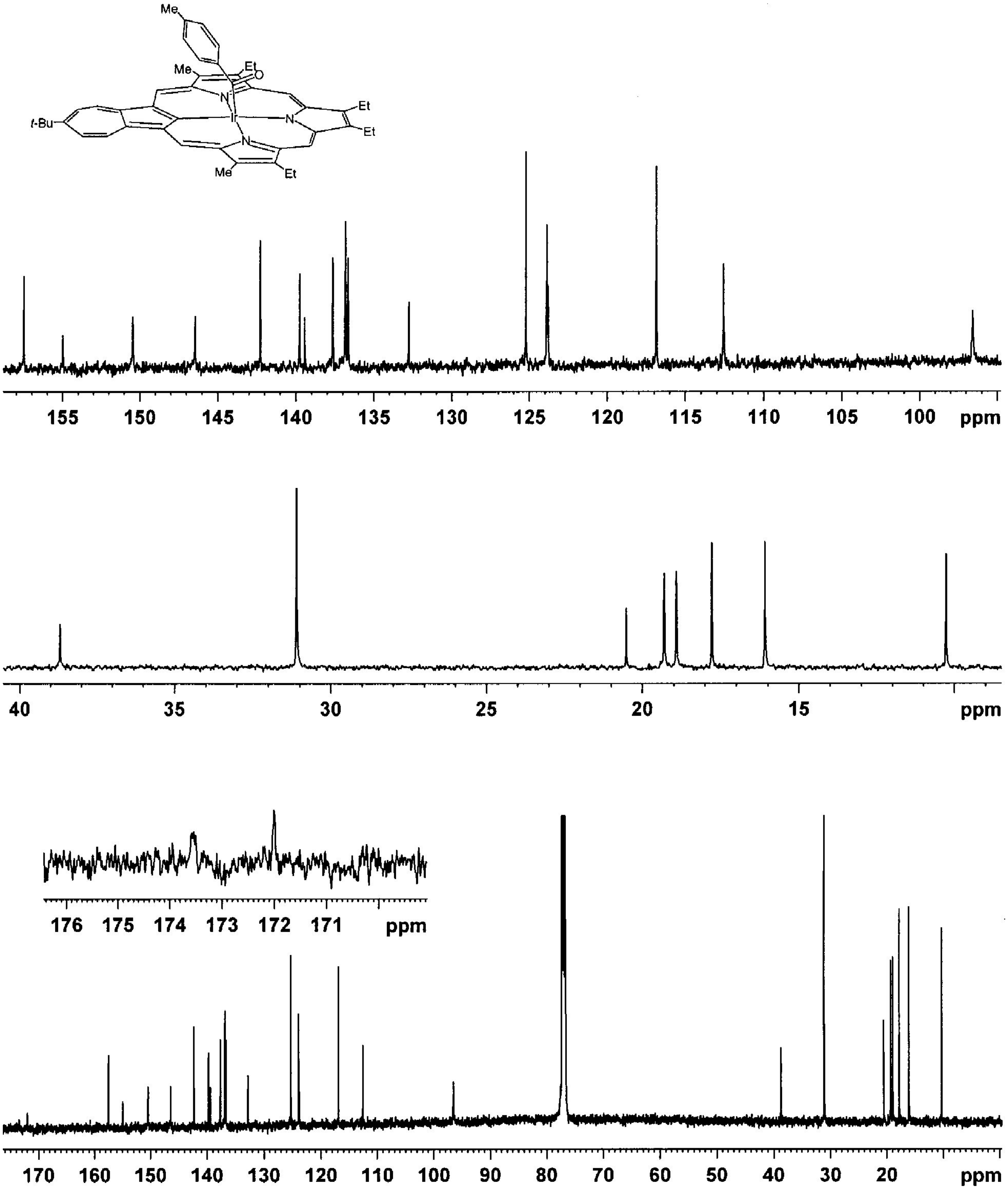

Figure S14. 125 MHz carbon-13 NMR spectrum of iridium(III) complex **11c** in $CDCl_3$ at 25 °C.

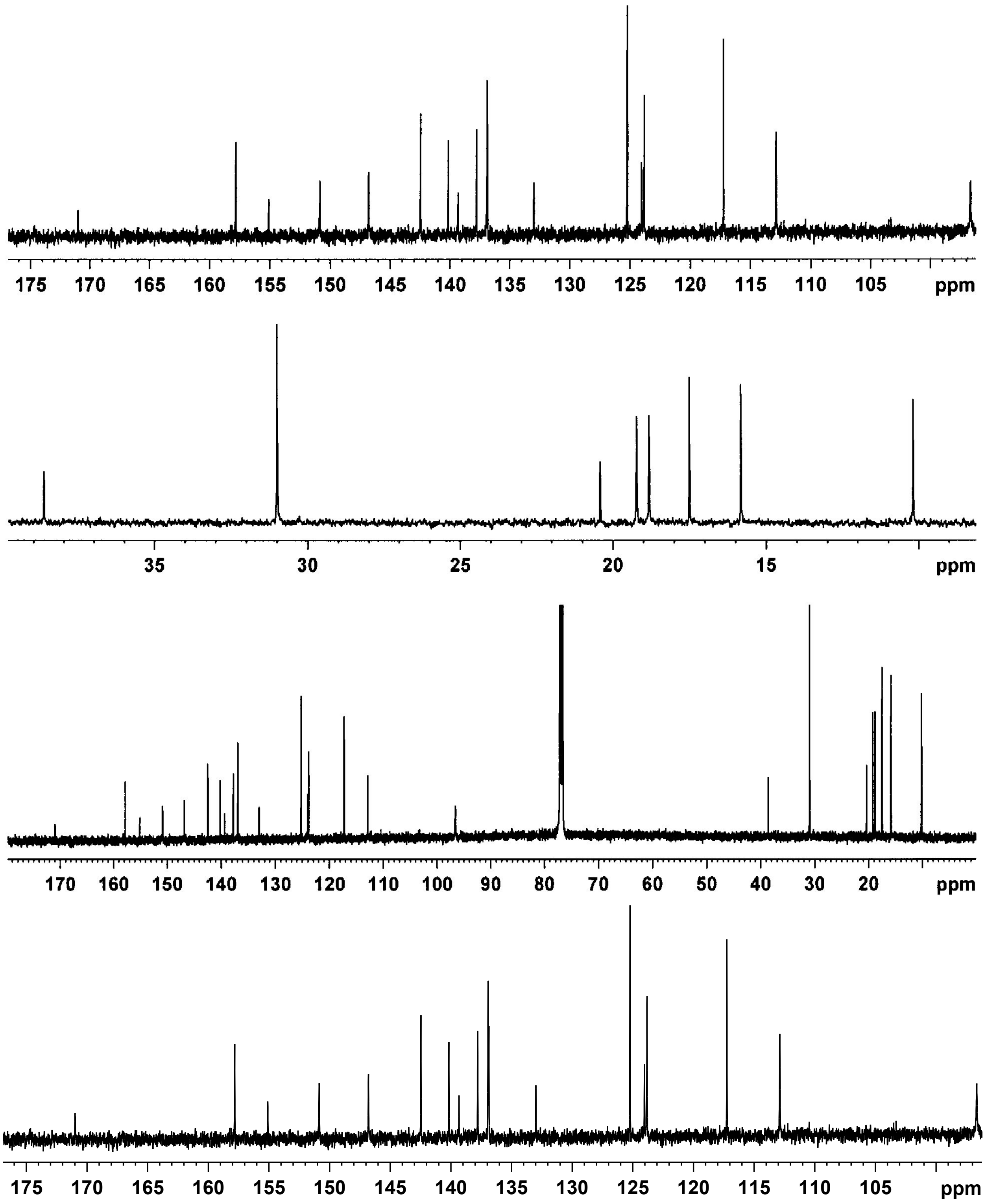

Figure S15. 125 MHz carbon-13 NMR spectrum of iridium(III) complex **11c** in $CDCl_3$ at 50 °C.

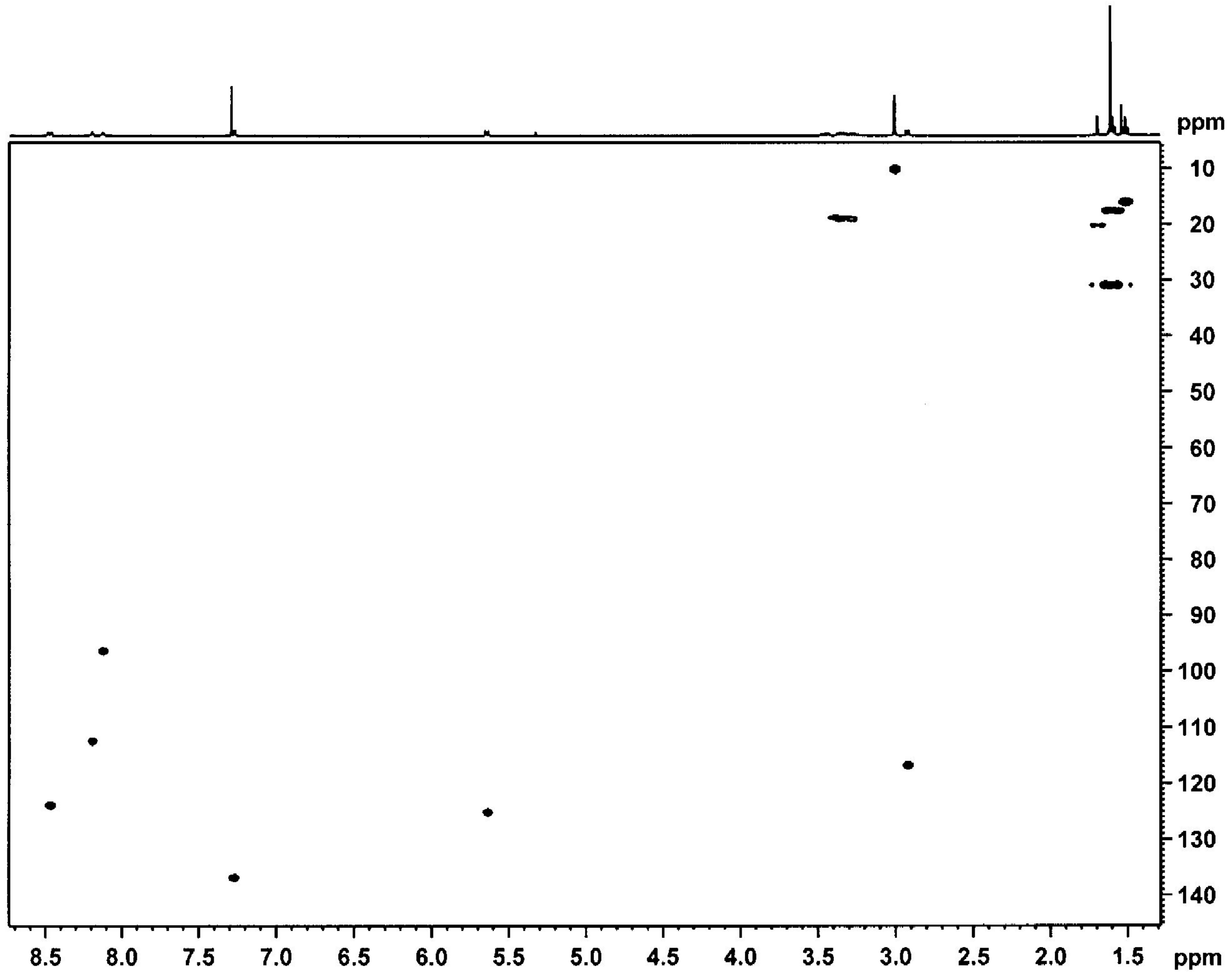

Figure S16. HSQC NMR spectrum of iridium(III) complex **11c** in $CDCl_3$.

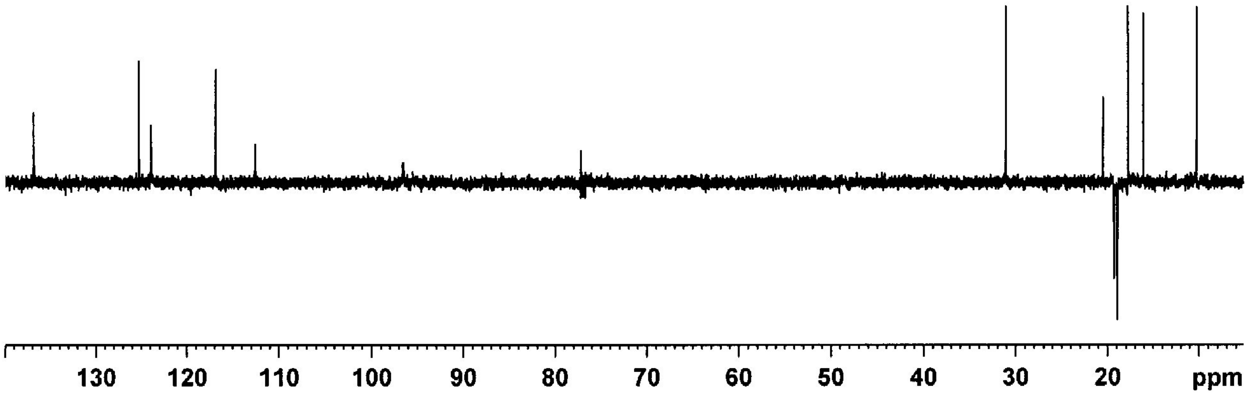

Figure S17. DEPT-135 NMR spectrum of iridium(III) complex **11c** in $CDCl_3$.

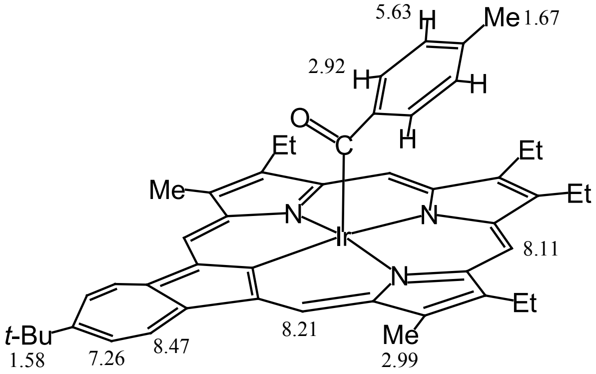

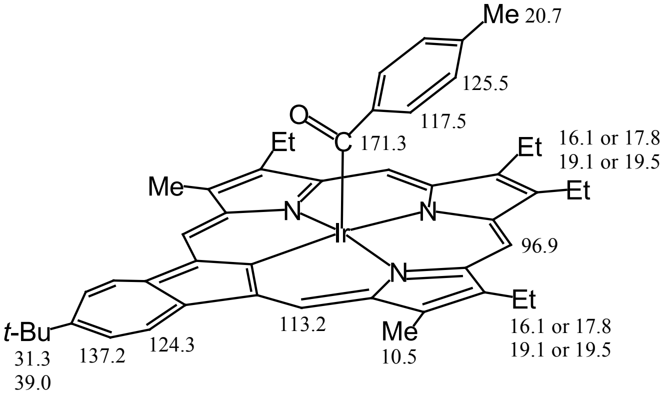

Figure S18. Partial assignment of the proton and carbon-13 NMR spectra for **11c** based on the foregoing data.

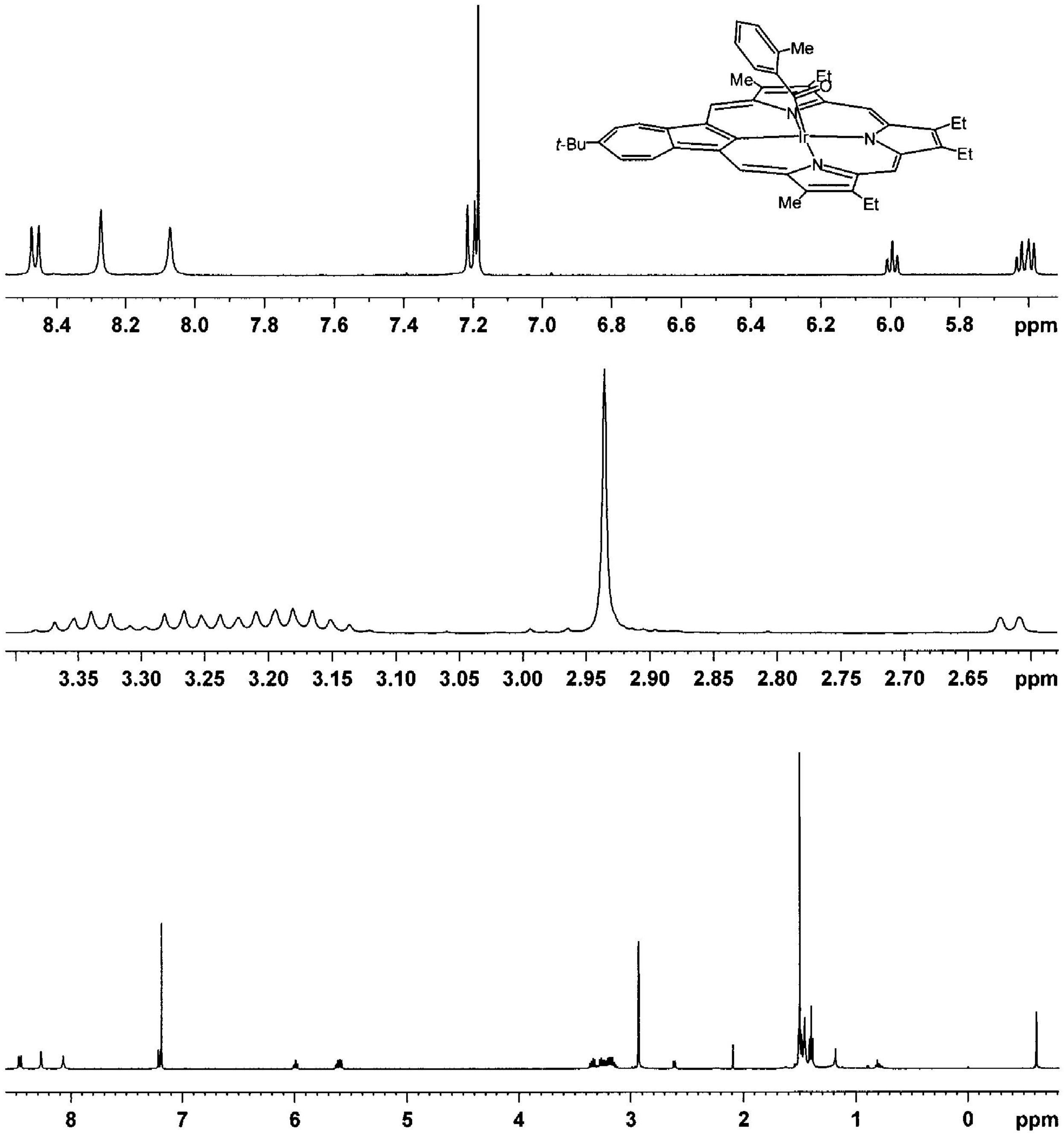

Figure S19. 500 MHz proton NMR spectrum of iridium(III) complex **11d** in $CDCl_3$ at 25 °C.

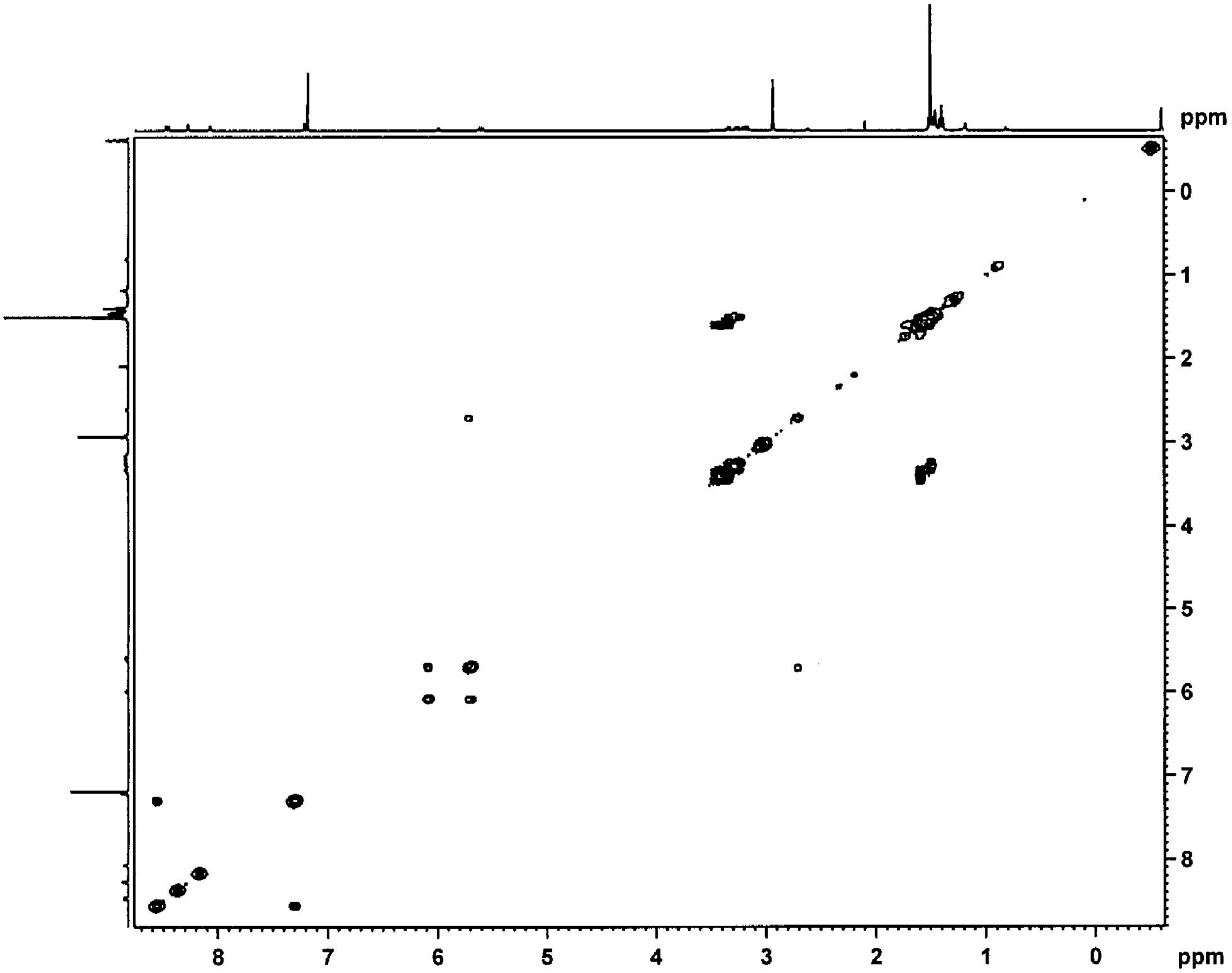

Figure S20. ^{1}H-^{1}H COSY NMR spectrum of iridium(III) complex **11d** in $CDCl_3$.

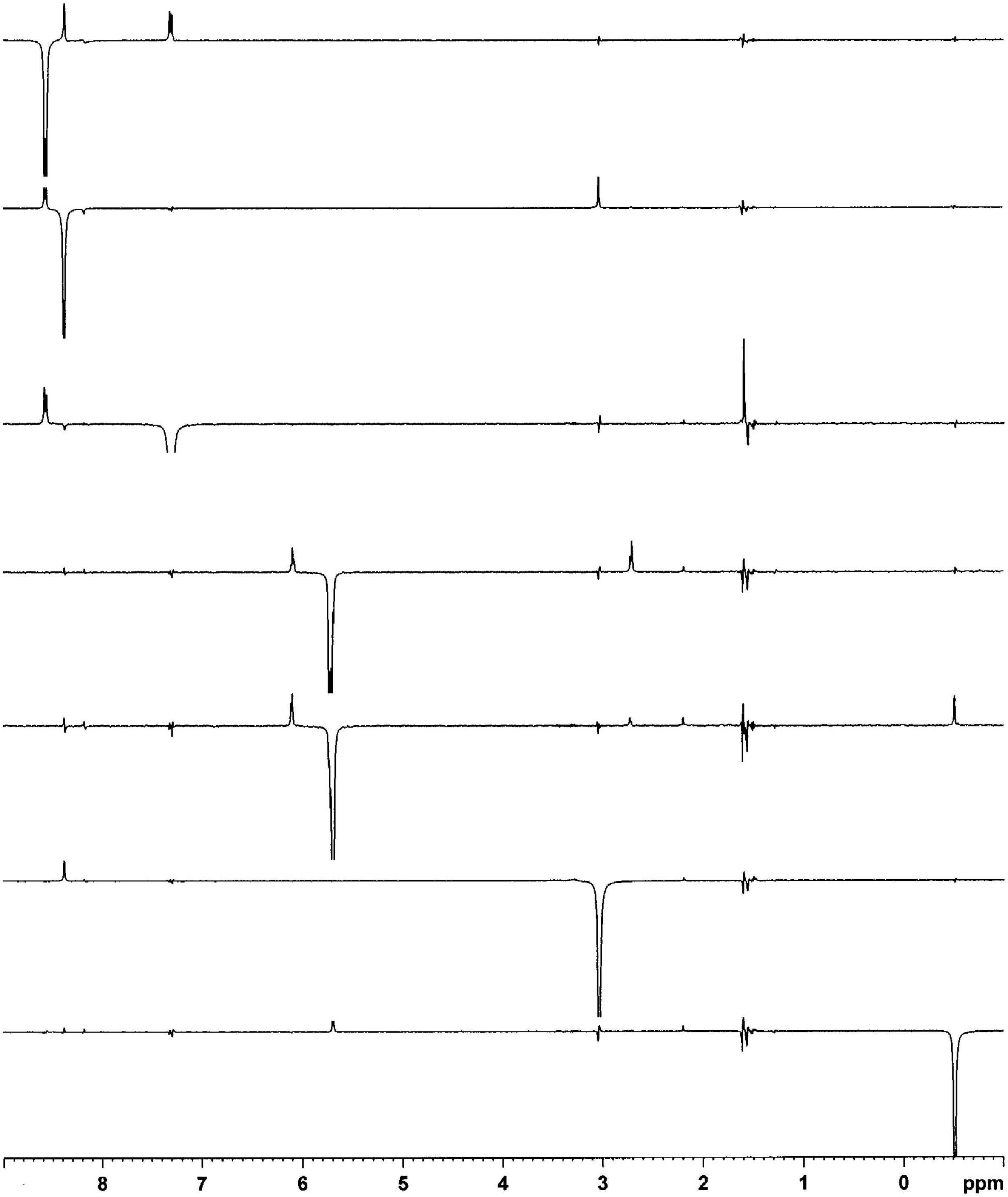

Figure S21. Selected nOe difference proton NMR spectra of iridium(III) complex **11d** in $CDCl_3$.

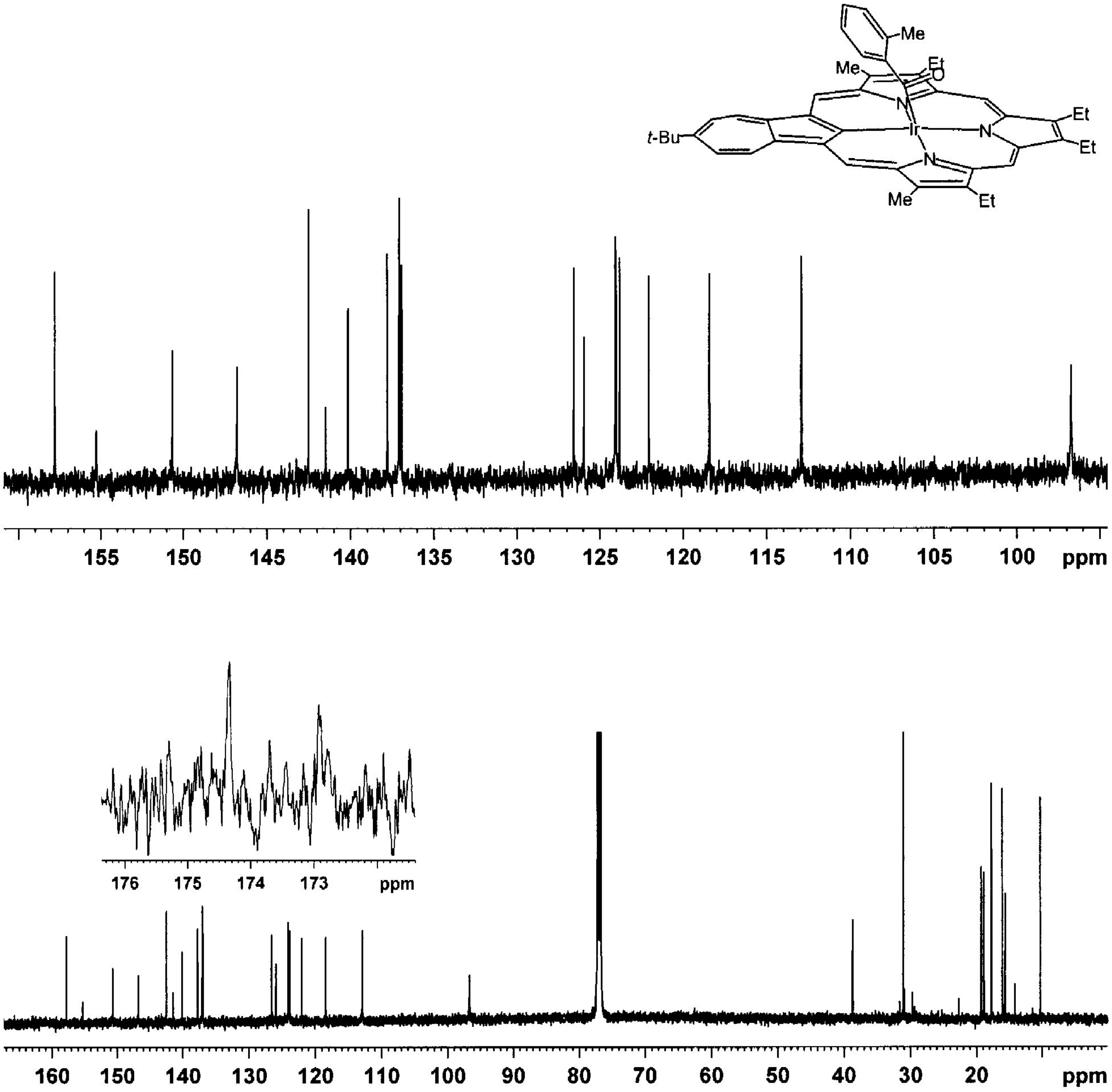

Figure S22. 125 MHz carbon-13 NMR spectrum of iridium(III) complex **11d** in $CDCl_3$.

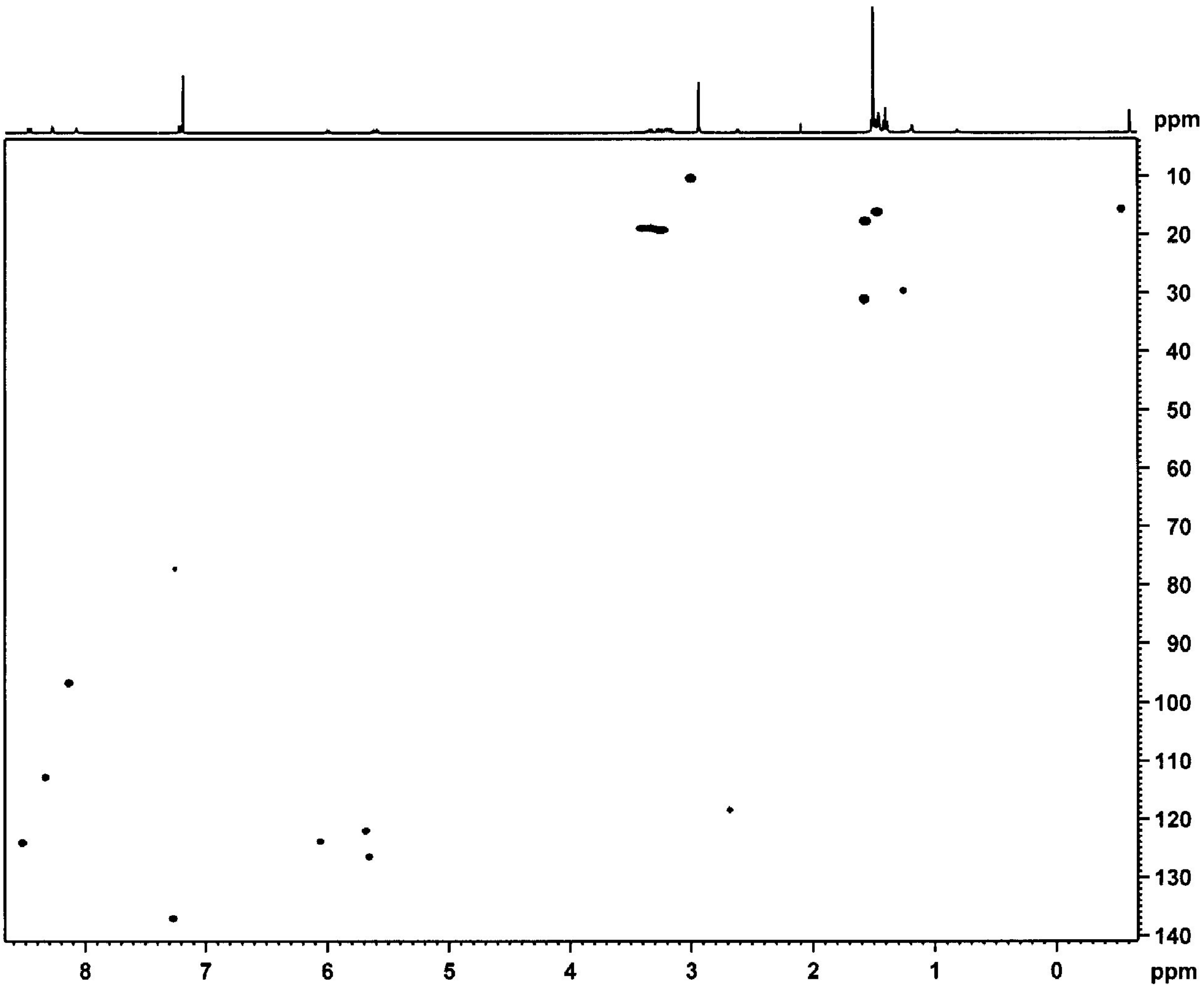

Figure S23. HSQC NMR spectrum of iridium(III) complex **11d** in $CDCl_3$.

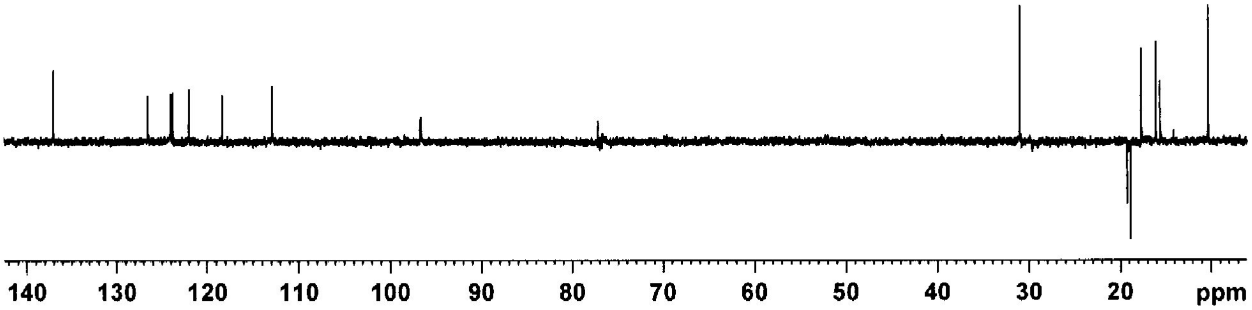

Figure S24. DEPT-135 NMR spectrum of iridium(III) complex **11d** in $CDCl_3$

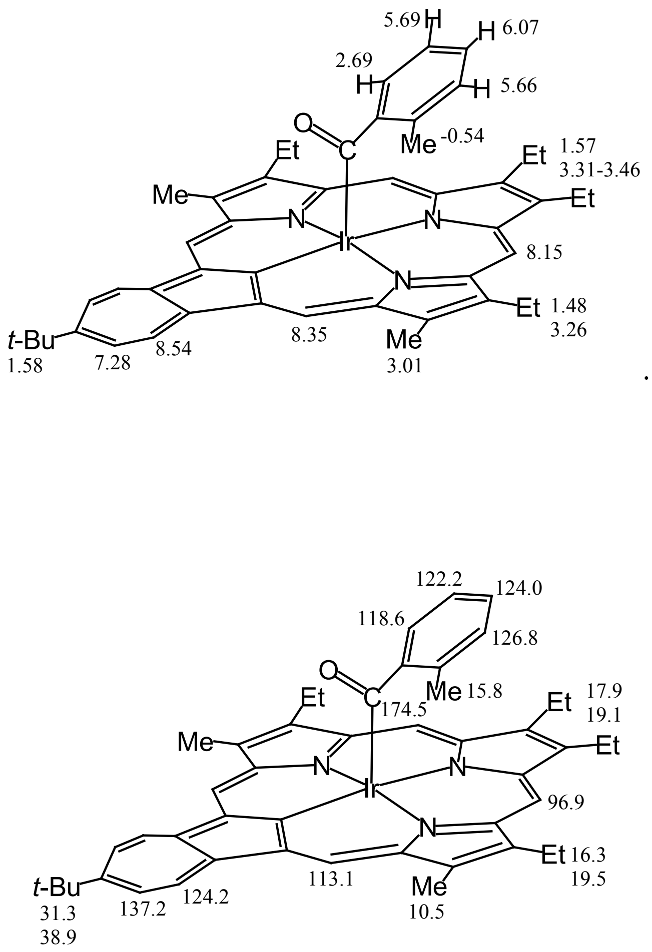

Figure S25. Partial assignment of the proton and carbon-13 NMR spectra for **11d** based on the foregoing data.

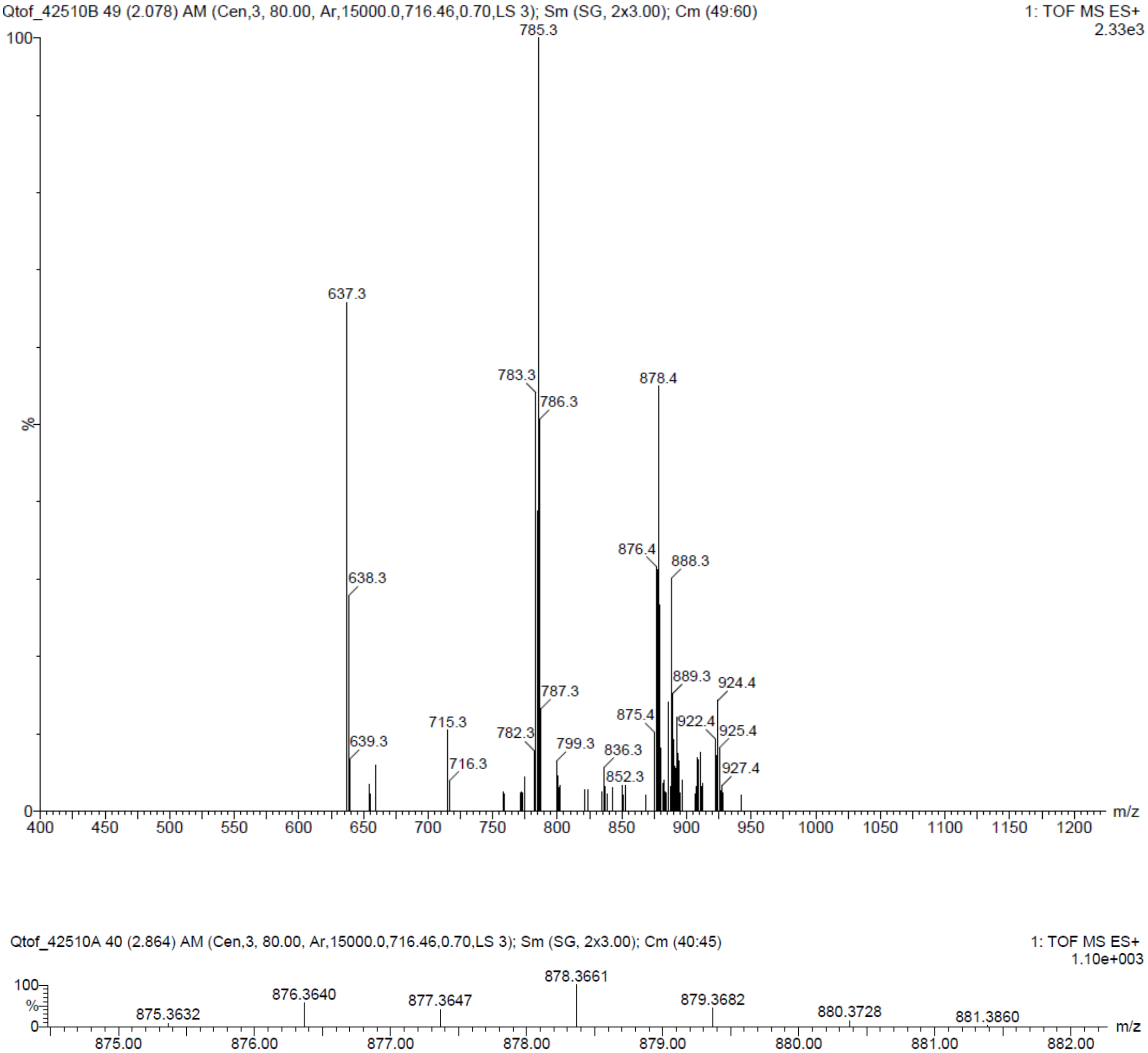

```
Minimum:                                  -1.5
Maximum:                  5.0      10.0   600.0

Mass       Calc. Mass     mDa      PPM    DBE      i-FIT      Formula

878.3661   878.3662       -0.1     -0.1   26.0     4.9        C48  H51  N3  O   Ir
           878.3675       -1.4     -1.6   25.5     5.7        C50  H53  O2  Ir
           878.3635       2.6      3.0    21.5     3.1        C45  H53  N2  O4  Ir
           878.3621       4.0      4.6    22.0     3.4        C43  H51  N5  O3  Ir
           878.3720       -5.9     -6.7   17.0     3.6        C41  H55  N3  O6  Ir
           878.3595       6.6      7.5    17.5     4.0        C40  H53  N4  O6  Ir
           878.3747       -8.6     -9.8   21.5     3.8        C44  H53  N4  O3  Ir
```

Figure S26. Electrospray ionization mass spectrum of iridium(III) complex **11c**.

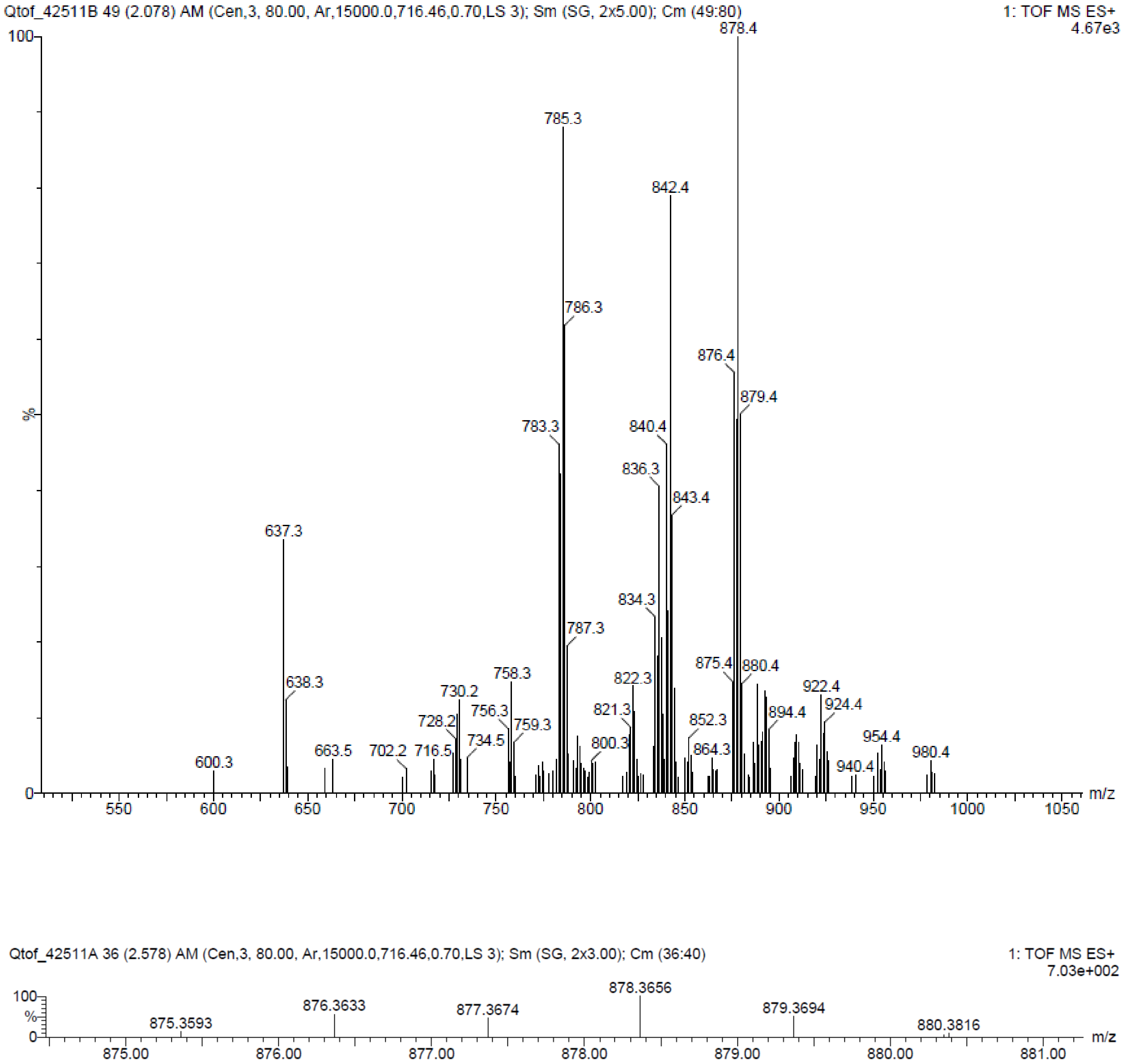

```
Minimum:                                      -1.5
Maximum:                     5.0      10.0    600.0

Mass       Calc. Mass        mDa      PPM     DBE       i-FIT      Formula

878.3656   878.3662          -0.6     -0.7    26.0      7.7        C48  H51  N3  O  Ir
           878.3675          -1.9     -2.2    25.5      9.9        C50  H53  O2  Ir
           878.3635          2.1      2.4     21.5      5.5        C45  H53  N2  O4  Ir
           878.3621          3.5      4.0     22.0      4.2        C43  H51  N5  O3  Ir
           878.3595          6.1      6.9     17.5      19.2       C40  H53  N4  O6  Ir
           878.3720          -6.4     -7.3    17.0      4.3        C41  H55  N3  O6  Ir
```

Figure S27. Electrospray ionization mass spectrum of iridium(III) complex **11d**.